Proc. Natl. Acad. Sci. USA
Vol. 89, pp. 9257–9261, October 1992
Biochemistry

Escherichia coli biotin holoenzyme synthetase/*bio* repressor crystal structure delineates the biotin- and DNA-binding domains

KEITH P. WILSON*†, LISA M. SHEWCHUK*, RICHARD G. BRENNAN*‡, ANTHONY J. OTSUKA§, AND BRIAN W. MATTHEWS*

*Institute of Molecular Biology, Howard Hughes Medical Institute and Department of Physics, University of Oregon, Eugene, OR 97403; and §Department of Biological Sciences, Illinois State University, Normal, IL 61761-6901

Contributed by Brian W. Matthews, July 1, 1992

ABSTRACT **The three-dimensional structure of BirA, the repressor of the *Escherichia coli* biotin biosynthetic operon, has been determined by x-ray crystallography and refined to a crystallographic residual of 19.0% at 2.3-Å resolution. BirA is a sequence-specific DNA-binding protein that also catalyzes the formation of biotinyl-5′-adenylate from biotin and ATP and transfers the biotin moiety to other proteins. The level of biotin biosynthetic enzymes in the cell is controlled by the amount of biotinyl-5′-adenylate, which is the BirA corepressor. The structure provides an example of a transcription factor that is also an enzyme. The structure of BirA is highly asymmetric and consists of three domains. The N-terminal domain is mostly α-helical, contains a helix–turn–helix DNA-binding motif, and is loosely connected to the remainder of the molecule. The central domain consists of a seven-stranded mixed β-sheet with α-helices covering one face. The other side of the sheet is largely solvent-exposed and contains the active site. The C-terminal domain comprises a six-stranded, antiparallel β-sheet sandwich. The location of biotin binding is consistent with mutations that affect enzymatic activity. A nearby loop has a sequence that has been associated with phosphate binding in other proteins. It is inferred that ATP binds in this region, adjacent to the biotin. It is proposed that the binding of corepressor to monomeric BirA may promote DNA binding by facilitating the formation of a multimeric BirA–corepressor–DNA complex. The structural details of this complex remain an open question, however.**

The biotin operon repressor, BirA, is a 33.5-kDa protein that regulates transcription of the *Escherichia coli* biotin operon (1–3). BirA is bifunctional, serving both as the biotin (vitamin H)-activating enzyme and as a transcriptional regulator. It catalyzes the formation of biotinyl-5′-adenylate from biotin and ATP and transfers biotin to a specific lysine residue on the biotin carboxyl carrier protein, a subunit of acetyl-CoA carboxylase (4, 5). If all the biotin-accepting proteins in the cell have been biotinylated, the BirA–biotinyl-5′-AMP complex accumulates and binds to the 40-base-pair *bio* operator, repressing transcription of the biotin biosynthetic genes (4, 6–8). Thus BirA synthesizes its own corepressor, a unique property among known DNA-binding proteins. BirA represses transcription when biotinyl-5′-AMP is bound to the enzyme, suggesting that binding of corepressor helps form the BirA–DNA complex.

Structure Determination

Crystals of BirA were grown as described (9) and equilibrated with 2.05 M phosphate, pH 6.5/5% (vol/vol) glycerol. Native and derivative data sets were collected by using film or a Xuong–Hamlin (10) area detector (Table 1). Inclusion of anomalous data in cross-phased difference Fourier maps showed the space group to be $P4_32_12$ rather than its enantiomorph.

Refined heavy-atom parameters were employed to compute multiple isomorphous replacement phases to 3.0-Å resolution. The mean figure of merit, including anomalous scattering data, was 0.62 to 3.0-Å resolution. The electron density map calculated with these phases could be interpreted for about 75% of the molecule. Cycles of model building, refinement (12), and phase combination served to improve the map. The current map is consistent with the derived amino acid sequence of BirA (6) and the chemical nature of the heavy-atom substitutions. The model (Fig. 1) has an *R* factor of 19.0% against all observed data between 20- and 2.3-Å resolution, with root-mean-square deviation from ideal bond lengths and bond angles of 0.013 Å and 2.4°, respectively. It includes 287 of the 321 amino acids in the repressor sequence (see below) and 44 bound solvent molecules. The distribution of ϕ and ψ angles is shown in Fig. 2.¶

Description of the Structure

Domain I. The BirA monomer has approximate dimensions of 75 Å × 35 Å × 30 Å and is organized in three domains (Fig. 1 *Left*). The N-terminal domain (residues 1–60) consists of three α-helices [A (residues 4–15), B (22–29), and C (33–46)] packed against two strands of antiparallel β-sheet [1 (49–54) and 2 (56–60)]. Sequence comparisons with members of the DNA-binding helix–turn–helix family suggested that residues 22–46 of BirA constituted a helix–turn–helix motif (13). The structure determination confirms that α-helices B and C correspond to the helix–turn–helix motif. The α-carbon atoms of residues 22–42 of BirA superimpose on α-carbons 16–36 of Cro protein from phage λ (14) with root-mean-square discrepancy of 0.91 Å. The discrepancy between residues 22–42 of BirA with residues 169–189 of the catabolite gene activator protein (15) is 0.67 Å. These values correspond well with the agreement between other known helix–turn–helix motifs (16, 17). The tenuous coupling of the DNA-binding domain to the rest of the protein suggests that large-scale conformational changes could easily occur both in solution and on binding DNA.

Domain II. The topology of the central domain of BirA (Fig. 1 *Left*) appears to be novel. A comparison with proteins in the Brookhaven Data Bank using the method of Subbarao and Haneef (18) revealed no corresponding structural fold. The domain consists of five α-helices [D (residues 68–76), E (89–97), F (147–164), G (234–256), and H (259–269)] and a mixed β-sheet consisting of seven strands [3 (80–84), 4 (104–

The publication costs of this article were defrayed in part by page charge payment. This article must therefore be hereby marked "*advertisement*" in accordance with 18 U.S.C. §1734 solely to indicate this fact.

†Present address: Vertex Pharmaceuticals Inc., 40 Allston Street, Cambridge, MA 02139.
‡Present address: Department of Biochemistry and Molecular Biology, Oregon Health Sciences University, 3181 SW Sam Jackson Park Road, Portland, OR 97201.
¶The atomic coordinates and structure factors have been deposited in the Protein Data Bank, Chemistry Department, Brookhaven National Laboratory, Upton, NY 11973 (reference P1BIA, P1BIB).

Table 1. Data collection and heavy-atom statistics

Protein modification	Data collection method	Resolution, Å	Completeness of data, %	R_{merge}, %	Unit cell dimensions, Å		No. of sites	R_c	Phasing power
					a,b	*c*			
Native	Film	20.0–2.3	70	7.5	114.0	60.2	—	—	—
Native	X-H	20.0–2.6	82	3.8	113.7	59.8	—	—	—
bioK	X-H	20.0–2.8	91	4.9	114.1	60.0	—	—	—
*p*CMB	X-H	20.0–3.0	73	4.2	114.4	59.9	2	0.67	0.71
$IrCl_3$	X-H	20.0–3.0	96	4.7	113.9	59.3	3	0.70	1.07
cis-Pt	X-H	20.0–3.0	96	4.1	114.1	60.0	4	0.68	1.42
DANP	X-H	20.0–3.8	93	7.5	114.0	60.2	3	0.70	0.75
$PtCl_4$	X-H	20.0–4.0	98	6.8	114.4	59.6	5	0.67	1.31

bioK is biotinylated lysine (1-day soak, saturated). *p*CMB is *p*-chloromercuribenzoic acid (3-day soak, saturated), $IrCl_3$ is iridium(III) chloride (2-day soak, 10.0 mM), Cis-Pt is *cis*-platinum(II)diammine dichloride (5-day soak, saturated), DANP is diaminodinitroplatinum (20-hr soak, 10% saturated solution), and $PtCl_4$ is platinum tetrachloride (1-day soak, 5.0 mM). Data were collected by an oscillation method (film) or on a Xuong–Hamlin (X-H) area detector (10). The number of heavy-atom binding sites is indicated where appropriate. The platinum compounds shared common sites but with different relative occupancies. R_{merge} gives the agreement between repeated intensity measurements, R_c is the Cullis *R* factor for centrosymmetric reflections, and the phasing power is the ratio of the average heavy-atom scattering to the average lack of closure of the phase triangles (11).

109), 5 (129–139), 6 (170–173), 7 (175–180), 8 (182–192), and 9 (200–210)]. The two parallel strands are inaccessible to solvent, as is strand 5. The remainder of the sheet has one face largely solvent-exposed and contains the active site (Fig. 1).

Domain II contains four loops, which appear to be mobile or unstructured and cannot be visualized in electron density maps. These loops occur in pairs in the three-dimensional structure (Fig. 1 *Left*). One disordered loop (residues 116–124) contains the sequence GRGRRG, previously identified as a consensus sequence (GXGXXG) associated with ATP binding (19, 20). In the nearby unstructured region (residues 212–223), limited proteolysis has revealed a subtilisin-sensitive bond that is partially protected from cleavage in the presence of corepressor (Dorothy Beckett, personal communication). This also suggests that this region of the protein is at or close to the site of binding of corepressor.

Domain III. Domain III is comprised of two three-stranded antiparallel β-sheets that cross each other at an angle of about

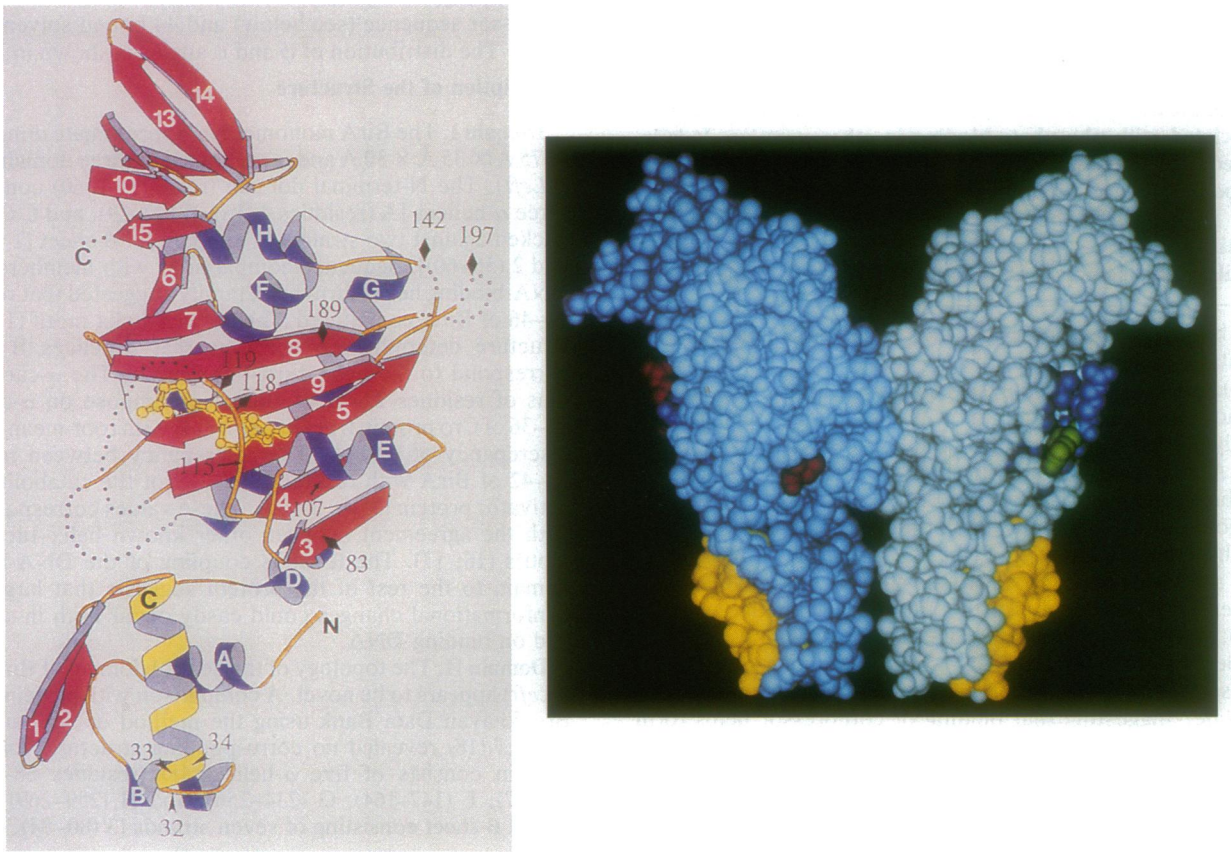

FIG. 1. (*Left*) Ribbon drawing showing the overall topology of the biotin repressor. α-Helices are colored blue and identified (A, B, . . .) according to their position in the primary sequence. β-Sheets are colored red and identified (1, 2, . . .). The relationship between the DNA recognition helix (yellow) and biotin (also yellow) is depicted. The locations of mutations that influence DNA binding (arrowheads) and enzymatic activity (arrows) are shown. Mutations that can be complemented and may form part of the proposed dimer interface are indicated by diamonds. (*Right*) Relationship between helix–turn–helix units (yellow), biotin binding sites (dark blue), and complementation sites (sites in green partially complement those in red) in a pair of BirA monomers related by the crystallographic dyad axis (vertical). It seems unlikely, but is not excluded, that the dimer as shown persists in solution.

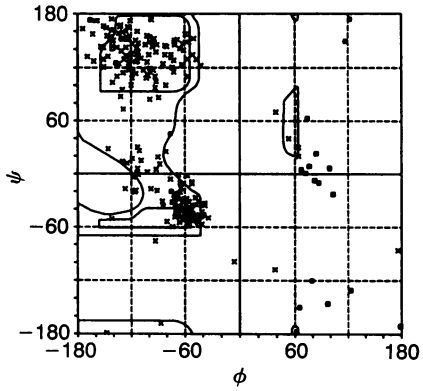

FIG. 2. Ramachandran diagram showing the distribution of ϕ and ψ angles for the refined model of the biotin repressor. Glycine residues are indicated by squares and non-glycines by crosses.

75° (Fig. 1 *Left*). Strands 10–15 make up this structure [10 (residues 274–280), 11 (283–287), 12 (288–293), 13 (296–302), 14 (305–309), and 15 (313–317)] and form a β-sandwich that caps one end of the biotin repressor.

The Biotin Binding Site

Exposure of BirA crystals to biotin or corepressor resulted in severe cracking and crystal destruction. This suggests that a conformational change accompanies corepressor binding. Because BirA transfers biotin to a specific lysine residue of biotin carboxyl carrier protein, attempts were also made to soak crystals of BirA with biotinylated lysine, and these proved to be successful in locating the biotin binding site (Fig. 3 *Top*). Coordinates of the complex were refined to a crystallographic residual of 17.3% at 2.8-Å resolution. Average deviations in bond lengths and angles from ideal values were 0.015 Å and 2.7°, respectively.

Biotin occupies a portion of the β-sheet face that is exposed to solvent in domain II, and makes contacts with parts of three β-strands (strands 5, 8, and 9), the N terminus of helix E, and main-chain atoms of residues 114–118 (Fig. 1 *Left*). Residues 116–118 are disordered in the apoprotein. Upon biotin binding they become localized and partially bury the biotin. The biotin binding pocket has hydrophobic sides with a more hydrophilic center. The biotin carbonyl and ureido nitrogens interact via hydrogen bonding with the hydrophilic interior of the cavity, while the hydrophobic tail and thiophene ring interact with the hydrophobic sides of the pocket. The thiophene ring contacts glycine residues 186, 204, and 206 (Fig. 3 *Middle* and *Bottom*). An absence of side chains at these three positions permits the thiophene ring to sit on a hydrophobic, relatively flat binding site. The bound biotin is less enclosed and appears to have less hydrophobic interaction with surrounding protein than is the case in the very tight complex of biotin with streptavidin (21, 22).

Specificity is derived from several hydrogen bonds between the biotin and the protein (Fig. 3 *Middle*). Particularly striking are the hydrogen bonds from the amide nitrogen of Arg-116 to the carbonyl oxygen of the biotin molecule, and from the carbonyl oxygen of Arg-116 to one of the biotin ureido nitrogens. In this instance the hydrogen bond donors and acceptors on the biotin participate in hydrogen bonds with the protein that are characteristic of β-sheet structure. There is also a hydrogen bond between the biotin carbonyl oxygen and the side-chain oxygen of Ser-89. The remaining ureido nitrogen participates in bidentate hydrogen bonds with the side-chain oxygen atoms of Thr-90 and Gln-112. The carboxyl group at the end of the hydrocarbon tail hydrogen bonds to the amino group of Lys-183. Upon biotin binding Glu-190 changes its χ_1 value by 115° and forms a salt bridge with Arg-116.

The ATP Binding Site

No direct crystallographic evidence for the ATP binding site has been obtained to date. Several lines of evidence, however, suggest that ATP will bind adjacent to the biotin. (*i*) ATP and biotin must be spatially close to permit the formation of biotinyl-5′-adenylate from biotin and ATP. (*ii*) Biotin binding orders the N-terminal portion of the presumed phosphate-binding loop. (*iii*) Mutations that affect enzymatic activity map to the region of the biotin binding site.

Correlation with Mutant Data

Mutants of the biotin repressor have been used to identify regions of the protein that are presumed to be involved in DNA binding, enzymatic activity, and/or protein dimerization (4, 6, 13). A subset of these is summarized in Table 2. In most cases knowledge of the three-dimensional structure permits rationalization of the observed phenotype. At the same time, the location of the mutation sites helps confirm the interpretation of the electron density map.

Regions of BirA likely to interact with DNA are suggested by mutants that inactivate repressor function but have little effect on enzymatic activity (13). Such mutations are restricted to three adjacent residues, amino acids 32–34 (Table 2), which had been predicted on the basis of sequence homology to occur in a helix–turn–helix motif (13). The three-dimensional structure shows that these three amino acids are located within the first turn of the recognition helix (Fig. 1 *Left*). The substitutions are ≈40 Å away from the biotin binding site, consistent with the observation that they have little effect on enzymatic activity. The remaining amino acid substitutions in Table 2 that are defective in repression (residues 118, 119, 142, and 197) are located at least 20 Å away from the DNA recognition helix. These mutations could disrupt direct communication between the corepressor binding site and the DNA-binding domain, or they might have a more indirect effect such as interference with protein dimerization that accompanies DNA binding (see below).

Mutations that affect the enzymatic activity of BirA occur at residues 107, 115, and 189 (Table 2), which are within 10 Å of the crystallographically determined biotin binding site (Fig. 1 *Left*). The side chain of Cys-107 is buried in the three-dimensional structure with its sulfur atom in van der Waals contact (3.9 Å) with the γ-methyl group of Thr-90. The γ-oxygen of Thr-90 in turn makes a hydrogen bond to the biotin. The Cys-107 → Gly substitution could disrupt this bond. Gly-115 is adjacent to the residues that become ordered upon biotin binding. The side chain of a non-glycine at residue 115 would protrude directly into the biotin binding site. Replacing Val-189 with glycine could affect the formation of the salt bridge between Glu-190 and Arg-116 that accompanies biotin binding.

Mutations in BirA that prevent growth at elevated temperatures presumably destabilize the protein. These mutations are located at positions 83, 142, 207, and 235, which are distributed throughout the three-dimensional structure. Val-83 is completely shielded from solvent. Its replacement with glycine would be expected to decrease hydrophobic and van der Waals interactions. Ile-207 is completely buried in the three-dimensional structure. Its replacement with serine presumably would place a hydrophilic amino acid within the protein core and so reduce stability. Arg-235 is involved in a solvent-inaccessible ion pair with Glu-110 and its replacement with cysteine would disrupt this salt bridge.

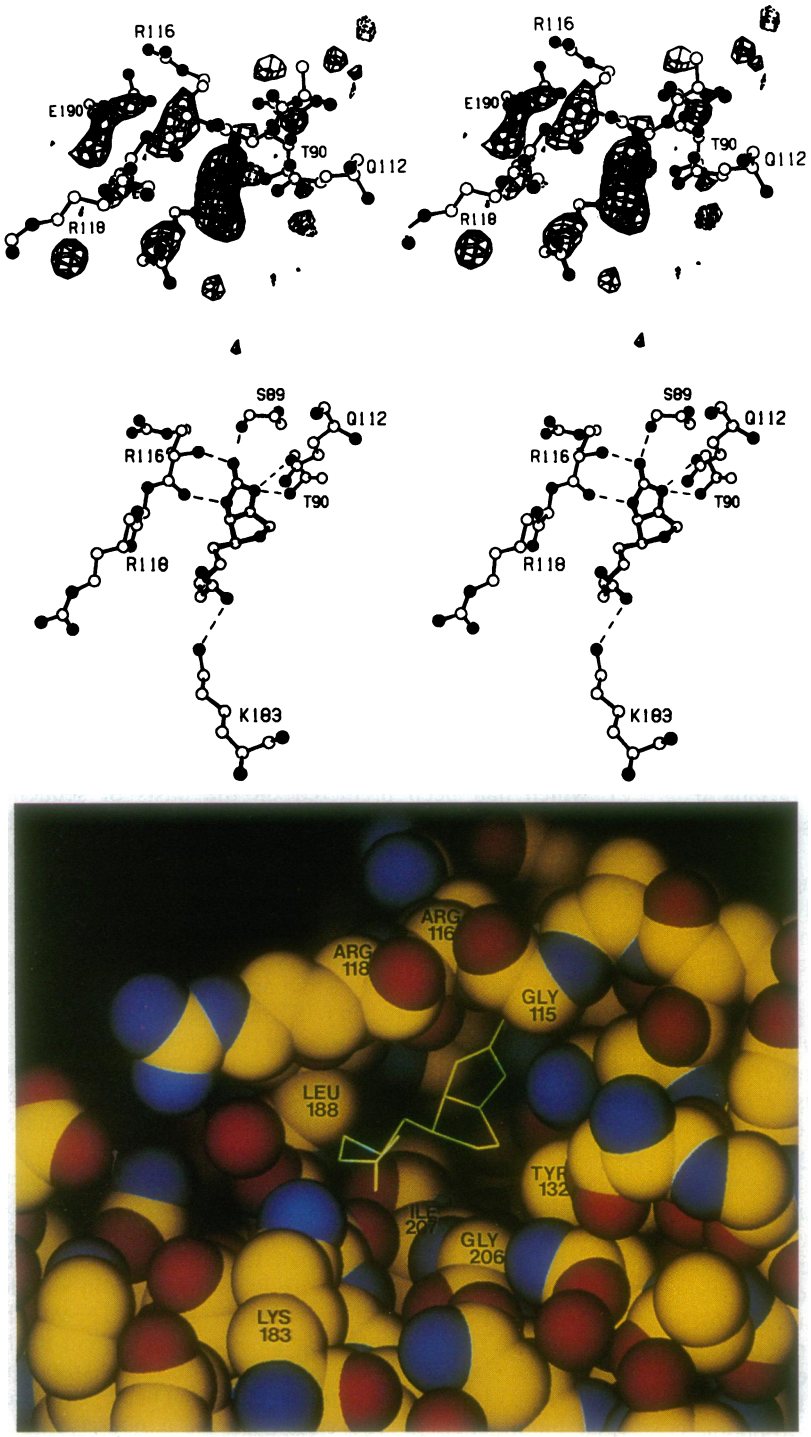

FIG. 3. (*Top*) Stereo map showing the difference in electron density between crystals of BirA soaked in biotinylated lysine and crystals of the apoprotein. A saturating amount (3.5 mg/ml) of biotinylated lysine (bioK) (Fluka) was dissolved in 2.05 M sodium potassium phosphate/5% glycerol, pH 6.5. One large crystal (0.6 mm × 0.4 mm × 0.4 mm) was soaked overnight in this solution and used to collect three-dimensional diffraction data to 2.8-Å resolution. Similar results were obtained with crystals soaked in the competitive inhibitor biotin methyl ester. Two significant positive difference peaks were found in each case, one corresponding to the biotin moiety and the other corresponding to several amino acids that become ordered upon biotin binding. Coefficients are $|F_{bioK} - F_{apo}|$ and phases are from the refined coordinates of the apoprotein. Positive contours (solid lines) and negative contours (broken lines) are drawn at levels of ± 3.0 σ, where σ is the root-mean-square density throughout the unit cell. The refined coordinates of the structure in the presence of biotinylated lysine are superimposed. Oxygen and sulfur atoms are drawn solid, carbon atoms open, and nitrogen atoms partially shaded. Amino acids are identified by their one-letter codes and by sequence position. No evidence for the location of the lysine portion of the biotinylated lysine was observed. (*Middle*) Stereo view of the hydrogen bonds (dashed lines) between the biotin molecule and BirA. Carbon atoms are drawn as open circles, oxygen and sulfur atoms are drawn solid, and nitrogen atoms are partially shaded. Amino acids are identified by their one-letter codes and by sequence position. Hydrogen bond distances are as follows: Arg-116 N to biotin O, 2.8 Å; Arg-116 O to biotin N3, 3.0 Å; Ser-89 O^{γ} to biotin O, 2.9 Å; Thr-90 O^{γ} to biotin N1, 2.8 Å; Gln-112 O^{ϵ} to biotin N1, 2.9 Å. (*Bottom*) Space-filling representation of the biotin binding pocket. Oxygen atoms are colored red, nitrogens blue, and carbons yellow. The biotin molecule is represented as a stick figure. Residues around the biotin pocket are identified.

Repression by BirA

Many helix–turn–helix DNA-binding proteins are dimeric and bind to their operators with twofold-related recognition helices occupying successive major grooves of the DNA (e.g., refs. 14 and 23–27). There are, however, several indications that BirA may not follow this pattern. First, the operator site for BirA is extended, encompassing 40 or so base pairs (4, 7, 8, 28). Also, experiments using analytical gel filtration chromatography and equilibrium analytical ultracentrifugation indicate that BirA remains monomeric in 50 mM Tris Cl/200 mM KCl/2.5 mM $MgCl_2$ at pH 7.5 and 20°C at concentrations ranging from 0.25 to 30 μM (Dorothy Beckett, personal communication). These concentrations are well above those at which specific binding to the biotin operator occurs. In the crystal structure, two adjacent monomers of BirA are in contact and are related by a twofold axis of symmetry (Fig. 1 *Right*). Because the area of contact is 1100 Å^2, substantially less than the 1600 Å^2 of buried surface area expected for dimeric proteins with subunit molecular masses in the 24- to 40-kDa range (29), the crystal contact may not represent a dimer contact in solution. While partial complementation of different *birA* alleles has been taken to suggest that a multimeric form may be involved in repression (4), none of the known complementation sites occurs at the crystal contact described above.

One way to at least partially integrate the data available at the present time is to assume that BirA oligomerizes as it binds to DNA. It was recently demonstrated that binding of BirA monomers to DNA is cooperative (Dorothy Beckett,

Table 2. Mutants of BirA (adapted from ref. 13)

Allele	Repression (1 mM biotin)	Complementation	Mutation position	Amino acid substitution
		Defective in repression		
birA361	−	ND	32	Ser → Arg
birA106	−	ND	32	Ser → Ile
birA825	−	ND	33	Arg → Leu
birA331	−	ND	34	Ala → Glu
birA91	−	A	118	Arg → Gly
birA352	−	B	119	Arg → Trp
birA71	−	ND	142	Gly → Cys
birA301	−	B	197	Asp → Tyr
		Mutations that map to the active-site region		
birA815	+	ND	107	Cys → Gly
birA1	+	ND	115	Gly → Ser
birA215	+	A	189	Val → Gly
		Temperature-sensitive phenotypes		
birA879	+	A	83	Val → Gly
birA71	−	ND	142	Gly → Cys
birA104	+	ND	207	Ile → Ser
birA85	−	ND	235	Arg → Cys

personal communication). Precedent for the oligomerization of a protein as it binds to DNA is provided by several examples (30, 31). In the case of BirA it would be assumed that the binding of corepressor favors formation of a dimeric or possibly multimeric complex of BirA on the operator. In such a complex the substitutions that complement one another (Table 2) might be spatially adjacent.

A second model involves restructuring upon ligand binding. In this case the formation of biotinyl-5′-adenylate on the catalytic domain would change the relative positions of the structural domains and would enhance affinity of monomeric BirA for DNA in some unspecified manner.

It is difficult, however, to predict the exact mode of alignment of BirA on DNA and so to differentiate between these and other possible models. Although the helix–turn–helix unit is usually well conserved in different helix–turn–helix DNA-binding proteins, the mode of interaction with DNA can vary substantially (23–27). The DNA can also bend to a greater or lesser degree (23–26). In the present case the apparent flexibility of the DNA-binding domain relative to the rest of the protein adds another uncertainty. A full understanding of the regulation of the biotin operon will require the crystal structure of the BirA–corepressor–DNA complex.

We thank Drs. Larry Weaver and William Tulip for help with data collection and other aspects, Dr. Dorothy Beckett for helpful discussions and for communicating results in advance of publication, and Drs. Allan M. Campbell and Max A. Eisenberg for comments on the manuscript. L.M.S. is a Fellow of the Jane Coffin Childs Memorial Fund for Medical Research. This work was supported in part by grants from the National Institutes of Health (GM31757 to A.J.O.; GM20066 to B.W.M.), the Jane Coffin Childs Memorial Fund for Medical Research, and the Lucille P. Markey Charitable Trust.

1. Eisenberg, M. A. (1984) *Ann. N.Y. Acad. Sci.* **447,** 335–349.
2. Otsuka, A. J., Buoncristiani, M. R., Howard, P. K., Matsuzaki, J., Ruppert, J., Shaw, J., Uchida, K. M. & Vasu, J. (1988) *Mol. Gen. (Life Sci. Adv.)* **7,** 131–134.
3. Cronan, J. E. (1989) *Cell* **58,** 427–429.
4. Barker, D. F. & Campbell, A. M. (1981) *J. Mol. Biol.* **146,** 451–467.
5. Eisenberg, M. A., Prakash, O. & Hsiung, S.-C. (1982) *J. Biol. Chem.* **257,** 15167–15173.
6. Howard, P. K., Shaw, J. & Otsuka, A. J. (1985) *Gene* **35,** 321–331.
7. Prakash, O. & Eisenberg, M. A. (1979) *Proc. Natl. Acad. Sci. USA* **76,** 5592–5595.
8. Cronan, J. E. (1988) *J. Biol. Chem.* **263,** 10332–10336.
9. Brennan, R. G., Sanjay, V., Matthews, B. W. & Otsuka, A. J. (1989) *J. Biol. Chem.* **264,** 5.
10. Xuong, N. H., Nielsen, C., Hamlin, R. & Anderson, D. (1985) *J. Appl. Crystallogr.* **181,** 342–350.
11. Blundell, T. L. & Johnson, L. N. (1976) *Protein Crystallography* (Academic, New York).
12. Tronrud, D. E., Ten Eyck, L. F. & Matthews, B. W. (1987) *Acta Crystallogr. A* **43,** 489–503.
13. Buoncristiani, M. R., Howard, P. K. & Otsuka, A. J. (1986) *Gene* **44,** 255–261.
14. Anderson, W. F., Ohlendorf, D. H., Takeda, Y. & Matthews, B. W. (1981) *Nature (London)***290,** 754–758.
15. McKay, D. B. & Steitz, T. A. (1981) *Nature (London)* **290,** 744–749.
16. Steitz, T. A., Ohlendorf, D. H., McKay, D. B., Anderson, W. F. & Matthews, B. W. (1982) *Proc. Natl. Acad. Sci. USA* **79,** 3097–3100.
17. Brennan, R. G. & Matthews, B. W. (1989) *J. Biol. Chem.* **264,** 1903–1906.
18. Subbarao, N. & Haneef, I. (1991) *Protein Eng.* **4,** 877–884.
19. Wierenga, R. K. & Hol, W. G. (1982) *Nature (London)* **302,** 842–844.
20. Schulz, G. E. (1992) *Curr. Opin. Struct. Biol.* **2,** 61–67.
21. Weber, P. C., Ohlendorf, D. H., Wendoloski, J. J. & Salemme, F. R. (1989) *Science* **243,** 85–88.
22. Hendrickson, W. A., Pähler, A., Smith, J. L., Satow, Y., Merritt, E. A. & Phizerlackerley, R. P. (1989) *Proc. Natl. Acad. Sci. USA* **86,** 2190–2194.
23. Jordan, S. R. & Pabo, C. O. (1988) *Science* **242,** 893–899.
24. Aggarwal, A. K., Rodgers, D., Drottar, M., Ptashne, M. & Harrison, S. C. (1988) *Science* **242,** 899–907.
25. Otwinowski, R. W., Schevitz, R. W., Zhang, R.-G., Lawson, C. L., Joachimiak, A., Marmorstein, R. Q., Luisi, B. F. & Sigler, P. B. (1988) *Nature (London)* **335,** 321–329.
26. Brennan, R. G., Roderick, S. L., Takeda, Y. & Matthews, B. W. (1990) *Proc. Natl. Acad. Sci. USA* **87,** 8165–8169.
27. Matthews, B. W. (1988) *Nature (London)* **335,** 294–295.
28. Otsuka, A. & Abelson, J. (1978) *Nature (London)* **276,** 689–693.
29. Miller, S., Lesk, A. M., Janin, J. & Chothia, C. (1987) *Nature (London)* **328,** 834–836.
30. Harrison, S. C. (1991) *Nature (London)* **353,** 715–719.
31. Kim, B. & Little, J. W. (1992) *Science* **255,** 203–206.